

## Normal-state optical conductivity of $\text{YBa}_2\text{Cu}_3\text{O}_{6+x}$

Badredine Arfi

*Department of Physics and Materials Research Laboratory, 1110 West Green Street, University of Illinois at Urbana-Champaign, Urbana, Illinois 61801*

(Received 14 June 1991)

The optical conductivity in the normal state of  $\text{YBa}_2\text{Cu}_3\text{O}_{6+x}$  is calculated within the framework of the memory-function formalism. We assume that the carriers are constrained to the  $\text{CuO}_2$  planes and are scattered by spin fluctuations of the Cu spins. First, the calculation is done using the phenomenological form of the spin susceptibility proposed in the antiferromagnetic-Fermi-liquid theory. In a second step, we choose two different forms of the spin susceptibility to improve the high-frequency dependence of the optical conductivity. It is found that fitting the experimental data requires more than one form of the spin susceptibility. It is also found that the relaxation rate varies roughly linearly with the frequency and that the mass enhancement is weakly frequency dependent.

### I. INTRODUCTION

Understanding the physical properties of the cuprate superconductors has remained a challenge to many condensed-matter theorists. Although a broad range of models and theories have been proposed<sup>1</sup> to date by many workers, none has successfully explained all available experimental data in either the normal state or the superconducting state. In the absence of a clear microscopic theory explaining the data, it is instructive to resort to phenomenological models to fit the experimental results with the hope of setting directions for more elaborate microscopic models.

Among the various proposed phenomenological approaches, the nearly-antiferromagnetic-Fermi-liquid theory proposed by Millis, Monien, and Pines<sup>2</sup> (MMP) seems to explain well the normal-state NMR data of different cuprate superconductors.<sup>3</sup> MMP argue that the various measurements in the normal state are consistent with a one-component system (i.e., one spin degree of freedom per  $\text{CuO}_2$  unit) of disordered but antiferromagnetically correlated spins, with the interpretation the spin system being the spin excitations of an antiferromagnetically correlated Fermi liquid. The two key assumptions in this approach are that the imaginary part of the spins susceptibility  $\chi''(q, \omega \rightarrow 0) \sim \omega$  at all  $q$ , where the momentum  $q$  is measured from the zone corner  $(\pi/a, \pi/a)$ , and that the antiferromagnetic correlations have relaxational dynamics.

In this paper we calculate the optical conductivity in the normal state of  $\text{YBa}_2\text{Cu}_3\text{O}_{6+x}$  ( $x=0.63, 1$ ) using three different models. The calculation is done using the memory-function formalism, which is well suited, since it permits one to define an effective frequency-dependent relaxation rate and mass enhancement making the comparison to experiment easy. A similar approach has been taken recently by Moriya and Takahashi.<sup>4</sup> We assume that the carriers are relaxed by scattering off the spin fluctuations of the nearly-antiferromagnetic Fermi liquid. In the first model, we use exactly the picture put forward

by MMP using their suggested form of the spin susceptibility. One drawback of this model is that it has been devised for NMR calculations, which are done at very small frequencies. Therefore, using exactly the same frequency dependence of  $\chi(q, \omega)$  when  $\omega$  is large may not be a good approximation. It is also clear that such a form of the susceptibility does not reproduce the experimental data on Raman scattering,<sup>5</sup> which are characterized by a roughly constant behavior for relatively large frequencies. The second model we propose is an attempt to include this important feature. In it we still keep the same characteristic spin-fluctuation energy  $\omega_{\text{SF}}$  as in MMP. The purpose of the third model is to relax this condition by taking a more generalized characteristic spin-fluctuation energy  $\bar{\omega}_{\text{SF}}$ , which is wave-vector dependent.

The experimental study of the optical properties in the normal state of  $\text{YBa}_2\text{Cu}_3\text{O}_7$  crystal has shown a number of anomalous features. Working with a single-domain crystal, Schlesinger *et al.*<sup>6</sup> found that the normal-state optical conductivity drops much more slowly with the frequency  $\omega$  than the ordinary Drude form. They were able to describe their data in terms of a scattering rate  $\hbar/\tau^* \sim k_B T + \hbar\omega$  at low frequency, where  $T$  is the temperature. In parallel to this, they found that the frequency-dependent effective mass changes from about 3 (in units of the bare mass) at very low frequencies to about 1 at frequencies of the order of  $2000 \text{ cm}^{-1}$ . Orenstein *et al.*<sup>7</sup> made a systematic study of the optical properties of  $\text{YBa}_2\text{Cu}_3\text{O}_{6+x}$ -based insulators and superconductors. They identified free carriers and interband contributions of  $\sigma(\omega)$ . These authors found that in metallic crystals the optical conductivity appears to contain at least two components, a narrow peak centered at  $\omega=0$  and a broad component that extends to  $\sim 2 \text{ eV}$ . The width of the narrow peak varies with temperature as  $\sim 2k_B T$ . They identified the narrow peak with part of the free-carrier component. They also concluded that there is an additional contribution to  $\sigma$  from free carriers in the frequency range of about  $\omega=0$  but below  $1 \text{ eV}$ . The frequency dependence of the free carriers they ex-

tract is not Drude-like and cannot be described by a single Lorentzian peak centered at  $\omega=0$ . They argued that the complicated frequency dependence of  $\sigma$  suggests that the free carriers interact significantly with some other excitations. They reported a mass enhancement of the order of 2–3. The overall physical picture they presented is as follows. At low frequency the translational motion of the quasiparticles is broadened by its weak coupling to low-energy excitations. At frequencies above 50 meV there is a second contribution to  $\sigma$ , which accounts for the majority of the spectral weight but cannot be explained by invoking inelastic scattering from a spectrum of dispersionless oscillators. Gao *et al.*<sup>8</sup> performed a study of far-infrared transmission and reflection of oriented  $\text{YBa}_2\text{Cu}_3\text{O}_{7-\delta}$  thin films. They argued that their results show a Drude response and mid-infrared absorption in the frequency range below  $350 \text{ cm}^{-1}$ . By fitting transmission data, they found the Drude relaxation rate to be linear in temperature, while the plasma frequency remains essentially constant. Their results show that the mid-infrared absorption is nearly temperature independent in both normal and superconducting states.

In Sec. II we briefly introduce the memory-function approach, and display results for the effective relaxation rate, mass enhancement, and optical conductivity in terms of the spin susceptibility  $\chi(q, \omega)$ . We discuss in Sec. III the three different models we consider. In Sec. IV we discuss our results and compare them to experiment and to other theoretical calculations. Finally, in Sec. V we give our conclusion.

## II. MEMORY FUNCTION APPROACH

The calculation of dynamical conductivity using the memory-function approach has been set on firm ground by Götze and Wölfle.<sup>9</sup> We shall closely follow their approach. We assume that we have a cylindrical Fermi surface in three dimensions or equivalently a circular Fermi surface in two dimensions. We neglect the contributions of impurities and phonons to the resistivity considering only the contribution of spin fluctuations. We also neglect contributions from interband processes and assume a one-band picture for the free carriers. Although the importance of interband contributions to the optical conductivity has been stressed in Ref. 7, we believe that the neglect of these processes is not a major drawback, since we are interested in looking at the importance of spin fluctuations and not the identification of all the processes that might be of some importance. The Hamiltonian of the system reads

$$H = H_0 + H_{\text{SF}} . \quad (1)$$

$H_0$  represents the free-band Hamiltonian of the carriers

$$K(\omega) = K_0 \sum_q q_x^2 \int_{-\infty}^{\infty} dz \chi''(q, z) \sum_k \frac{1}{z + \varepsilon_k - \varepsilon_{k+q} - \omega} [n(\varepsilon_{k+q} - \varepsilon_k) - n(z)] [f(\varepsilon_k) - f(\varepsilon_{k+q})] , \quad (12)$$

where  $n$  is the Bose function,  $f$  is the Fermi function, and  $K_0$  is a constant.  $\chi''(q, z)$  is the imaginary part of the spin susceptibility, which will be introduced phenomenologically in the next section. The imaginary part of the correlation function  $K(\omega)$  reads

$$H_0 = \sum_{p, \sigma} \varepsilon_p c_{p\sigma}^\dagger c_{p\sigma} , \quad (2)$$

where  $\varepsilon_p = (p^2 - p_F^2)/2m$ , and  $c_{p\sigma}^\dagger$  ( $c_{p\sigma}$ ) is the carrier-creation (annihilation) operator.  $H_{\text{SF}}$  is the Hamiltonian characterizing the scattering of the carriers by the spin fluctuations, and is given by

$$H_{\text{SF}} = \sum_{k, k'} \sum_{\sigma, \sigma'} J_{kk'} \mathbf{S} \cdot \mathbf{s}_{\sigma\sigma'} c_{k\sigma}^\dagger c_{k'\sigma'} , \quad (3)$$

where  $J_{kk'}$  is the interaction matrix element, which we take to be constant  $J_{kk'} = J$ ,  $\mathbf{S}$  is the spin of the intermediate boson, while  $\mathbf{s}$  is the spin of the carriers.

In linear-response theory, the dynamical conductivity is related to the current-current correlation function  $C(\omega)$  by

$$\sigma(\omega) = -i \frac{e^2}{\omega} C(\omega) + i \frac{\omega_p^2}{4\pi\omega} , \quad (4)$$

where  $\omega_p^2 = 4\pi e^2 n/m$  is the plasmon frequency. The correlation function is given by

$$C(\omega) = -i \int_0^\infty e^{i\omega t} \langle [J_x(t), J_x^\dagger] \rangle dt , \quad (5)$$

where the current reads

$$J_x = \sum_{k, \sigma} \frac{\partial \varepsilon_k}{\partial k_x} c_{k\sigma}^\dagger c_{k\sigma} . \quad (6)$$

The memory function<sup>9</sup> is introduced by the following equation:

$$M(\omega) = -i\omega C(\omega) / [C_0 - C(\omega)] , \quad (7)$$

where  $C_0$  is the static limit of  $C(\omega)$ . Equation (7), can be inverted to give

$$C(\omega) = C_0 M(\omega) / [-i\omega + M(\omega)] . \quad (8)$$

The function  $M(\omega)$  is well behaved for  $\omega \rightarrow 0$ . The dynamical conductivity  $\sigma(\omega)$  is given by

$$\frac{1}{\sigma(\omega)} = \frac{4\pi}{\omega_p^2} [M(\omega) - i\omega] . \quad (9)$$

The memory function  $M(\omega)$  is given by

$$M(\omega) = \frac{4\pi}{\omega_p^2} \frac{K(\omega) - K(0)}{i\omega} , \quad (10)$$

where  $K(\omega)$  is the function

$$K(\omega) = i \int_0^\infty dt e^{i\omega t} \langle [J_x(t), J_x^\dagger] \rangle , \quad (11)$$

with

$$\dot{J}_x = i[J_x, H_{\text{SF}}] .$$

A straightforward calculation of  $K(\omega)$  gives

$$\text{Im}K(\omega) = K_0 \sum_q q_x^2 \int_{-\infty}^{\infty} dz \chi''(q, z) F(q, \omega - z) [n(z) - n(z - \omega)], \quad (13)$$

where

$$F(q, \omega) = \pi \sum_k \delta(\epsilon_k - \epsilon_{k+q} - \omega) [f(\epsilon_{k+q}) - f(\epsilon_k)]. \quad (14)$$

In the following we will make the low-frequency approximation

$$F(\mathbf{q}, \omega) \approx F_0 \omega. \quad (15)$$

The real part of  $M(\omega)$  takes the form

$$M'(\omega) = \frac{4\pi}{\omega_p^2} \frac{\text{Im}K(\omega)}{\omega}, \quad (16)$$

that is

$$M'(\omega) \approx \frac{4\pi}{\omega_p^2} Q^2 F_0 K_0 \frac{1}{\omega} \sum_q \int_{-\infty}^{\infty} dz \chi''(\mathbf{q} + \mathbf{Q}, z) (\omega - z) [n(z) - n(z - \omega)]. \quad (17)$$

The imaginary part of  $M(\omega)$  is obtained as

$$M''(\omega) = \frac{1}{\pi} \mathbf{P} \int_{-\infty}^{\infty} d\nu \frac{M'(\nu)}{\nu - \omega}, \quad (18)$$

where  $\mathbf{P}$  is the Cauchy principal value.

To facilitate the comparison with experimental data we define an effective relaxation rate  $1/\tau^*(\omega)$  and an effective-mass enhancement  $m^*(\omega)/m$ , by writing the conductivity as<sup>9</sup>

$$\frac{1}{\sigma(\omega)} = \frac{4\pi}{\omega_p^2} \frac{m^*(\omega)}{m} \left[ \frac{1}{\tau^*(\omega)} - i\omega \right]. \quad (19)$$

Using Eqs. (9) and (19) we identify

$$\frac{m^*(\omega)}{m} = 1 - \frac{M''(\omega)}{\omega}, \quad (20)$$

and

$$\frac{1}{\tau^*(\omega)} = M'(\omega) / \left[ 1 - \frac{M''(\omega)}{\omega} \right]. \quad (21)$$

We find it useful to define another relaxation time  $\tau(\omega)$  by

$$\frac{1}{\tau(\omega)} = \frac{m^*(\omega)}{m} \frac{1}{\tau^*(\omega)}. \quad (22)$$

Using Eqs. (20)–(22), we obtain the zero-frequency result:

$$\frac{1}{\tau(0)} = M'(0),$$

so that the dc resistivity reads

$$\rho(T) = \frac{4\pi}{\omega_p^2} \frac{1}{\tau(T)} = \frac{4\pi}{\omega_p^2} M'(0).$$

We remark that  $M'(0)$  is finite as opposed to  $M''(0)$ , which vanishes identically. This fact is due to the causality property of the response function.<sup>9</sup> The zero-frequency mass enhancement is then given by

$$\frac{m^*(0)}{m} = 1 - \frac{\partial}{\partial \omega} M''(\omega) \Big|_{\omega=0}$$

### III. SPIN SUSCEPTIBILITIES

In this section we introduce the three spin susceptibilities that will be used in Eq. (17) to calculate the memory function.

#### A. Antiferromagnetic paramagnon model (model A)

The first model we consider is that used by MMP to analyze the NMR experimental data. The spin-spin correlation function near the antiferromagnetic wave vector  $\mathbf{Q} = (\pi/a, \pi/a)$  is assumed to take the form

$$\chi(\mathbf{q} + \mathbf{Q}, \omega) = \frac{\chi_Q(T)}{1 + \xi^2 q^2 - i\omega/\omega_{\text{SF}}}, \quad (23)$$

where  $\chi_Q(T)$  is the static spin susceptibility at the antiferromagnetic wave vector  $\mathbf{Q}$ ,  $\xi$  is the antiferromagnetic correlation length, and  $\hbar\omega_{\text{SF}}$  is a typical energy scale for the antiferromagnetic paramagnons that describe the AF spin dynamics. This latter is related to the energy scale of the spin dynamics of the noninteracting system  $\Gamma$  by

$$\omega_{\text{SF}} = \frac{\Gamma}{\pi} \left[ \frac{a}{\xi} \right]^2 \frac{1}{\sqrt{\beta}}. \quad (24)$$

In Eq. (24)  $a$  is the lattice constant and  $\beta$  is a parameter that MMP determine by fitting the experimental results.  $\chi_Q(T)$  is related to  $\omega_{\text{SF}}$  by

$$\chi_Q(T) = \frac{\Gamma}{\pi \omega_{\text{SF}}} \frac{\chi_0}{1 + \sqrt{\beta}/2\pi^2}, \quad (25)$$

where  $\chi_0$  is the measured static susceptibility. From the best fits to data on  $\text{YBa}_2\text{Cu}_3\text{O}_7$ , MMP extract the values  $\beta \approx \pi^2$  and  $\Gamma \approx 0.4$  eV. They also find  $\omega_{\text{SF}} \sim T$ . For  $\text{YBa}_2\text{Cu}_3\text{O}_{6.63}$ ,  $\chi_0$  is strongly temperature dependent,<sup>10</sup> while Monien, Pines, and Takigawa<sup>3</sup> find that  $\Gamma$  is weakly temperature dependent. We use their results to predict the frequency dependence of the optical conductivity for  $\text{YBa}_2\text{Cu}_3\text{O}_{6.63}$ . The imaginary part of the spin susceptibility is given by

$$\chi''(\mathbf{q}+\mathbf{Q},\omega)=\chi_Q(T)\frac{\omega/\omega_{\text{SF}}}{(1+\xi^2q^2)^2+\frac{\omega^2}{\omega_{\text{SF}}}}. \quad (26)$$

For small frequencies we have

$$\chi''\sim\frac{\omega}{\omega_{\text{SF}}}\chi_Q/[1+\xi^2q^2]^2$$

and for high frequencies we have  $\chi''\sim\chi_Q(\omega_{\text{SF}}/\omega)$ .

It is clear that if one assumes the same susceptibility when calculating the Raman scattering intensity divided by the Bose factor, one runs into difficulty, since the intensity is  $\sim\chi''$  and experimentally the intensity is seen to be a flat function of the frequency shift for high frequency ( $\lesssim 2$  eV), whereas at small frequencies we obtain the right behavior. Consequently, one expects that the optical conductivity obtained in this case will be close to the experimental result for very low frequencies only.

### B. Model B

In view of the above comments, we consider an improved version of MMP's susceptibility by putting into it more frequency dependence but still preserving the linear behavior at small frequencies. We choose to replace the term  $\omega/\omega_{\text{SF}}$  in the expression of  $\chi(\mathbf{q}+\mathbf{Q},\omega)$  by the function  $\tanh(\omega/\omega_{\text{SF}})$ . It is clear that for  $\omega$  smaller than  $\omega_{\text{SF}}$  we will obtain the same qualitative behavior as in the paramagnon case. But for  $\omega > \omega_{\text{SF}}$  we have

$$\chi(\mathbf{q}+\mathbf{Q})\approx\chi_Q(T)\frac{1}{1-i+\xi^2q^2}. \quad (27)$$

This form, therefore, does comply with the experimental results of Raman scattering. It is to be remarked that this model is very close to the marginal-Fermi-liquid model with the added feature of  $q$  dependence.

In this model the characteristic spin-fluctuation energy is kept the same as in the paramagnon model and is, roughly speaking,  $\sim T$ . The other parameters are also kept the same.

### C. Model C

The two previous models can be improved in many directions. We choose, however, to consider the following physically motivated improvement. We would like the model susceptibility to allow for the fact that the spin fluctuations play a major role only in the region around the antiferromagnetic wave vector  $\mathbf{Q}$ . One way to simulate this is to make the characteristic spin-fluctuation energy dependent on the wave vector. To accomplish this goal we write the spin susceptibility in the following form:

$$\chi(\mathbf{q}+\mathbf{Q},\omega)=\frac{\chi_Q(T)}{1+\xi^2q^2}\frac{1}{1-i\tanh(\omega/\bar{\omega}_{\text{SF}})}, \quad (28)$$

where

$$\bar{\omega}_{\text{SF}}\equiv\bar{\omega}_{\text{SF}}(q)=\frac{\Gamma}{\pi\sqrt{\beta}}\left[\frac{a}{\xi}\right]^2(1+\xi^2q^2). \quad (29)$$

For  $q=0$  (at the antiferromagnetic wave vector) we obtain

$$\bar{\omega}_{\text{SF}}(0)=\frac{\Gamma}{\pi\sqrt{\beta}}\left[\frac{a}{\xi}\right]^2=\omega_{\text{SF}}, \quad (30)$$

but for  $q^2=|\mathbf{Q}|^2=2\pi^2/a^2$ , we have

$$\bar{\omega}_{\text{SF}}(\mathbf{Q})=2\pi\frac{\Gamma}{\sqrt{\beta}}\left[1+\frac{1}{2\pi^2}\left[\frac{a}{\xi}\right]^2\right]. \quad (31)$$

At  $T=100$  K, we have  $\xi\sim 3a$  so that  $\bar{\omega}_{\text{SF}}(\mathbf{Q})\approx 2\Gamma$ .

It should be remarked that for both cases B and C the sum rules are exhausted by choosing an appropriate high-frequency cutoff  $\omega_g$ . It is expected that the differences between the results of the three models will be mostly noticeable at relatively high frequencies. We point out that cases B and C possess features of both the antiferromagnetic-Fermi-liquid theory and the marginal-Fermi-liquid theory: in the former case at low frequencies, but in the latter case at both low and high frequencies. One can equally consider the proposed forms of  $\chi(\mathbf{q},\omega)$  as spin susceptibilities or charge polarizabilities or both at the same time.

## IV. RESULTS AND DISCUSSION

In this section we use the different susceptibilities proposed in the preceding section to calculate the memory function  $M(\omega)$ . To make our model calculation closer to reality we choose a cutoff for the sum over  $\mathbf{q}$  in Eq. (17) such that the area of the Fermi sea is equal to the magnetic Brillouin zone, which leads to a cutoff  $q_B=2\sqrt{\pi}/a$ .

The final results can be cast in the following form for all cases:

$$M'(\omega)=g\chi_0(T)T\frac{T}{\omega}I\left[\frac{\omega}{T}\right] \quad (32)$$

and

$$M''(\omega)=\frac{2}{\pi}g\chi_0(T)L\left[\frac{\omega}{T}\right], \quad (33)$$

where  $g$  is a quantity to be obtained from comparison to experimental data. The function  $L(\nu)$  is given by

$$L(\nu)=\text{P}\int_0^\infty\frac{du}{u^2-\nu^2}\frac{I(u)}{u}, \quad (34)$$

while the function  $I(u)$  takes a form specific to each susceptibility. In the case of the paramagnon model  $I(u)$  reads<sup>4</sup>

$$I(u) = 2\pi u [\phi(z/2\pi) - \phi(z_r/2\pi)] + u [\Lambda(z, u) - \Lambda(z_r, u)] \\ + \sum_{\sigma=\pm 1} \int_{-\infty}^{\infty} dx \frac{\sigma x}{e^x - 1} \left[ \tan^{-1} \left[ \frac{x + \sigma u}{z} \right] - \tan^{-1} \left[ \frac{x + \sigma u}{z_r} \right] \right], \quad (35)$$

where  $z = \omega_{\text{SF}}/T$ , and  $z_r = z(1+r)$ , with  $r = 4\Gamma/\omega_{\text{SF}}\sqrt{\beta}$ . The functions  $\phi$  and  $\Lambda$  are given, respectively, by

$$\phi(x) = \ln\Gamma(x) + x - (x - \frac{1}{2})\ln x - \ln\sqrt{2\pi}, \quad (36)$$

where  $\Gamma(x)$  is the gamma function, and

$$\Lambda(x, u) = \frac{u^2 - x^2}{2u} \tan^{-1} \frac{u}{x} - \frac{x}{2} \ln \left[ 1 + \frac{u^2}{x^2} \right] - \frac{x}{2}. \quad (37)$$

In the model B case,  $I(u)$  is given by

$$I(u) = u^2 \int_0^1 dx (1-x)t(xu) + 2u \int_0^{\infty} dx \frac{t(x)}{e^x - 1} + \sum_{\sigma=\pm 1} \int_0^{\infty} dx \frac{\sigma x}{e^x - 1} t(x + \sigma u), \quad (38)$$

where the function  $t(x)$  is defined as

$$t(x) = \tan^{-1} \left[ \tanh \left[ \frac{x}{z} \right] \right] - \tan^{-1} \left[ \frac{1}{1+r} \tanh \left[ \frac{x}{z} \right] \right]. \quad (39)$$

Finally, in model C,  $I(u)$  reads

$$I(u) = u^2 \int_0^1 dx (1-x)f(xu) + 2u \int_0^{\infty} dx \frac{f(x)}{e^x - 1} + \sum_{\sigma=\pm 1} \int_0^{\infty} dx \frac{\sigma x}{e^x - 1} f(x + \sigma u),$$

where  $f$  is defined as

$$f(x) = \int_{T_1(x)}^{T_2(x)} dt \frac{t}{2t^2 + 1} \frac{1}{\ln[t + (1+t^2)^{1/2}]}, \quad (41)$$

with

$$T_1(x) = \sinh \left[ \frac{x}{z} \right], \quad T_2(x) = \sinh \left[ \frac{x}{z(1+r)} \right]. \quad (42)$$

The zero-frequency result for the relaxation rate is

$$\frac{1}{\tau} = g\chi_0(T)TW(T), \quad (43)$$

where for the paramagnon case,  $W(T)$  is given by

$$W(T) = 2 \int_0^{\infty} dx \frac{xe^x}{(e^x - 1)^2} \left[ \tan^{-1} \left[ \frac{x}{z} \right] - \tan^{-1} \left[ \frac{x}{z(1+r)} \right] \right]. \quad (44)$$

For the model B case we have

$$W(T) = 2 \int_0^{\infty} dx \frac{xe^x}{(e^x - 1)^2} \left[ \tan^{-1} \left[ \tanh \frac{x}{z} \right] - \tan^{-1} \left[ \frac{1}{1+r} \tanh \frac{x}{z} \right] \right], \quad (45)$$

while in the model C case we obtain

$$W(T) = 2 \int_0^{\infty} dx \frac{xe^x}{(e^x - 1)^2} \int_{t_1(x)}^{t_2(x)} dt \frac{1}{t} \frac{\tanh t}{1 + \tanh^2 t}, \quad (46)$$

where

$$t_1(x) = \frac{x}{z}, \quad t_2(x) = \frac{x}{z(1+r)}. \quad (47)$$

The resistivity then takes the form

$$\rho(T) = \frac{4\pi}{\omega_p^2} g\chi_0(T)TW(T). \quad (48)$$

### A. $\text{YBa}_2\text{Cu}_3\text{O}_7$

In this subsection we compare our results to two sets of experimental data on two different  $\text{YBa}_2\text{Cu}_3\text{O}_7$  samples obtained by Schlesinger *et al.*<sup>6</sup> and Orenstein *et al.*<sup>7</sup>. The values of  $g$  that we obtained in the two cases are slightly different due to sample-dependence effects. (See Fig. 1.) First we start with the results of Ref. 7.

The two quantities we need to determine  $g$  are the resistivity due to the spin fluctuation  $\rho_{\text{SF}}(T_c)$  and the effective plasmon frequency  $\omega_p^*$ . The latter is related to

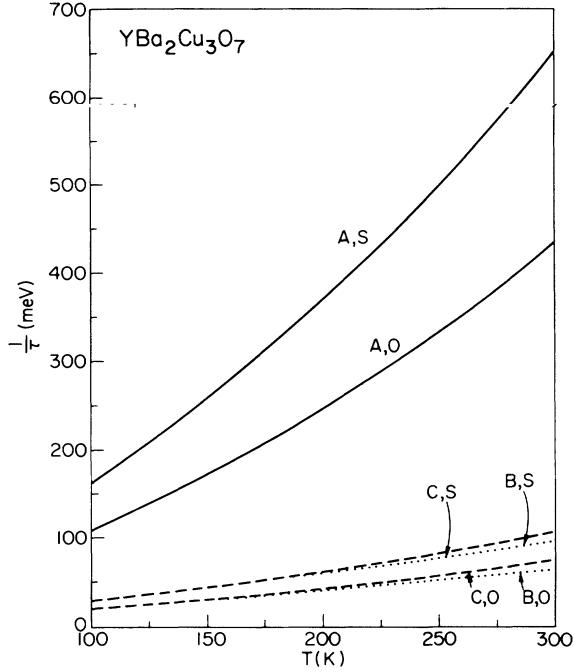


FIG. 1. Temperature dependence of the relaxation rate for models (A), (B), and (C) using either the set of  $g_s$  (S) or  $g_0$  (O) for  $\text{YBa}_2\text{Cu}_3\text{O}_7$ .

the bare plasmon frequency  $\omega_p^* = \omega_p m / m^*(0)$ . For  $\text{YBa}_2\text{Cu}_3\text{O}_7$ , Orenstein *et al.*<sup>7</sup> gave  $\omega_p^* \approx 1.5$  eV. The spin-fluctuation part of the resistivity  $\rho_{\text{SF}}$  is determined as

$$\rho_{\text{SF}}(T_c) = \rho(T_c) - \rho_{\text{imp}},$$

where  $\rho(T_c)$  is the measured resistivity at  $T = T_c$ , and  $\rho_{\text{imp}}$  is the residual resistivity at  $T = 0$  due to impurity scattering. From Ref. 7 we have  $\rho_{\text{imp}} = 10 \mu\Omega \text{ cm}$  and  $\rho(T_c) = 50 \mu\Omega \text{ cm}$ . We thus obtain  $\rho_{\text{SF}}(T_c) \approx 40 \mu\Omega \text{ cm}$  (we assume that the only relevant scattering mechanism is the spin-fluctuation one). We obtain the following values of  $g$ :

$$\begin{aligned} g_0 &= 0.58, \quad \text{paramagnon}, \\ g_0 &= 0.45, \quad \text{model B}, \\ g_0 &= 0.33, \quad \text{model C}, \end{aligned} \quad (49)$$

In the case of the results of Ref. 6, to determine  $g$ , we use the empirical formula given in that reference, i.e.,

$$\frac{\hbar}{\tau^*} = \alpha_s (\pi k_B T + \hbar\omega), \quad (50)$$

where  $\alpha_s \approx 0.6$ . We find

$$\begin{aligned} g_s &= 0.87, \quad \text{paramagnon}, \\ g_s &= 0.67, \quad \text{model B}, \\ g_s &= 0.47, \quad \text{model C}. \end{aligned} \quad (51)$$

The coefficient  $\alpha$  can be related to  $\omega_p^*$  and  $\rho_{\text{SF}}(T_c)$  in the following way:

$$\alpha = 1.64 \frac{(\omega_p^*)^2 \rho_{\text{SF}}(T_c)}{\pi T_c}, \quad (52)$$

where  $\omega_p^*$  is in units of eV,  $\rho_{\text{SF}}(T_c)$  in units of  $\mu\Omega \text{ cm}$ , and  $T_c$  in K. For the sample of Ref. 7, we obtain  $\alpha_0 \approx 0.52$ .

In Fig. 2 we display the frequency dependence of the effective relaxation rates obtained for the models A, B, and C using the respective  $g_s$ 's. The experimental result of Ref. 6 falls very close to the paramagnon result for  $T = 100$  K. The two other models (B and C) give results in qualitative agreement with Eq. (48). We should mention that our results for the paramagnon case differ from those of Ref. 4: we do not find any crossing between curves at different temperatures, while they did.

In Fig. 3, we plot the effective-mass enhancement as a function of frequency for the three models as well as the result of Ref. 6. Although there is a qualitative agreement between our results and the experimental data, we are unable to produce a quantitative fit as in the relaxation rate case. Nevertheless, we predict that the mass enhancement in the case of  $\text{YBa}_2\text{Cu}_3\text{O}_7$  material should decrease with increasing temperature.

In Figs. 4 and 5, we display the equivalent of Figs. 2 and 3 but for the quantity  $g$  determined by using the results of Ref. 7. The difference between the two cases is of a quantitative nature and not a qualitative one. In Fig. 6, we compare the optical conductivity at  $T = 200$  K we obtain for the three models with the result of Ref. 7. We see that at low frequencies ( $\omega \leq 20$  meV) the results of both models A and B fit the experimental data. At much higher frequencies, the model C result is closer to experimental data than the others. Although we do not display it, we find that the heights of  $\sigma(\omega)/\omega_p^2$  as a function of frequency for the three models appear to be  $\sim 1/T$  and the widths at half maximum height appear to be  $\sim 2T$ , which is in accordance with the results of Orenstein *et al.*<sup>7</sup>

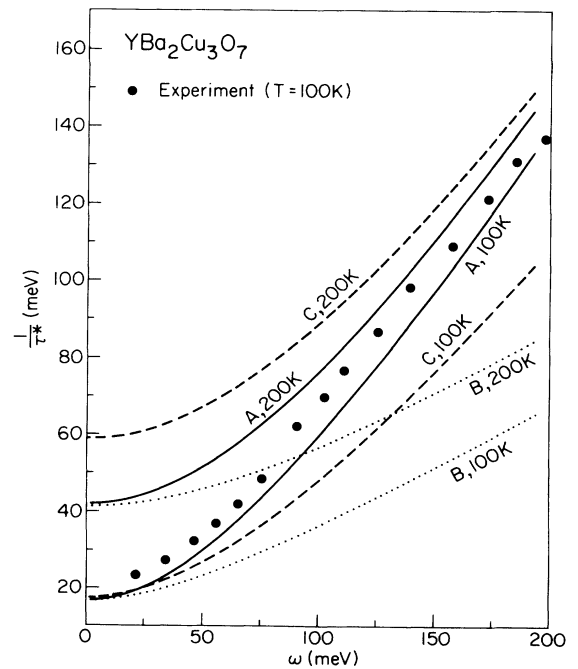


FIG. 2. Frequency dependence of the effective relaxation rate at  $T = 100$  and  $200$  K, compared to the experimental data of Ref. 6 for  $\text{YBa}_2\text{Cu}_3\text{O}_7$ .

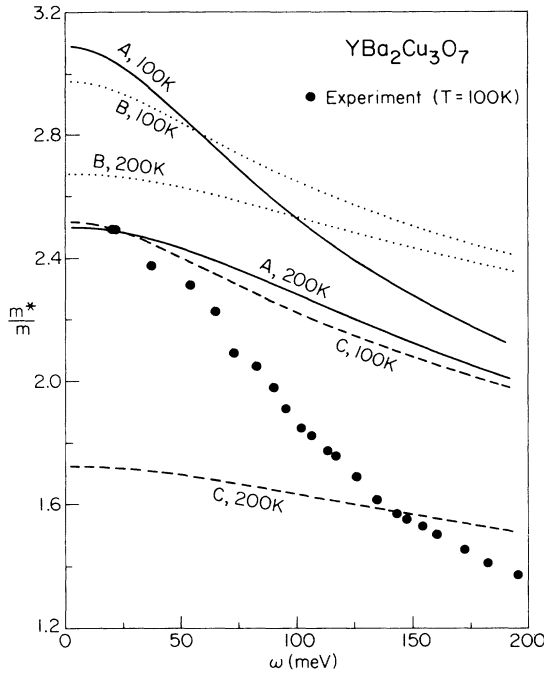


FIG. 3. Frequency dependence of the mass enhancement at  $T = 100$  and  $200$  K, compared to the experimental data of Ref. 6 for  $\text{YBa}_2\text{Cu}_3\text{O}_7$ .

As stated earlier, our results in the paramagnon case are comparable to those of Ref. 4, since the two models rely on the same physics. We should mention also that our results are in agreement with those obtained by Ruvalds and Virosztek<sup>11</sup> using the Fermi-surface nesting approach with the small difference that the mass enhance-

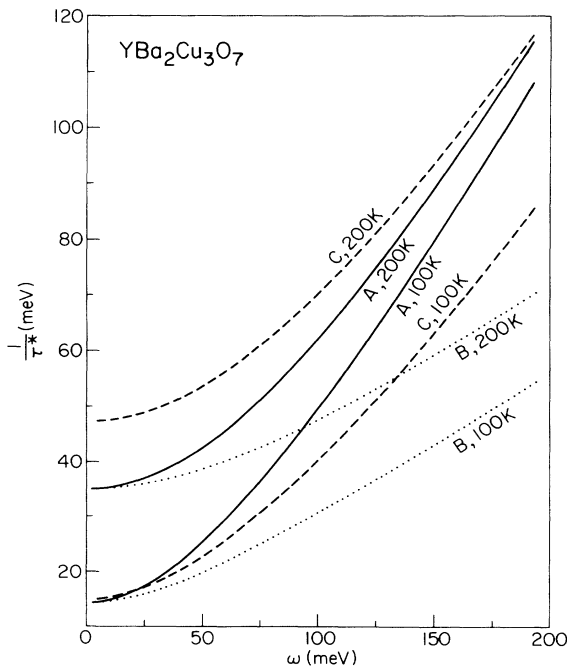


FIG. 4. Same as Fig. 2 but using  $g_0$  instead of  $g_s$ .

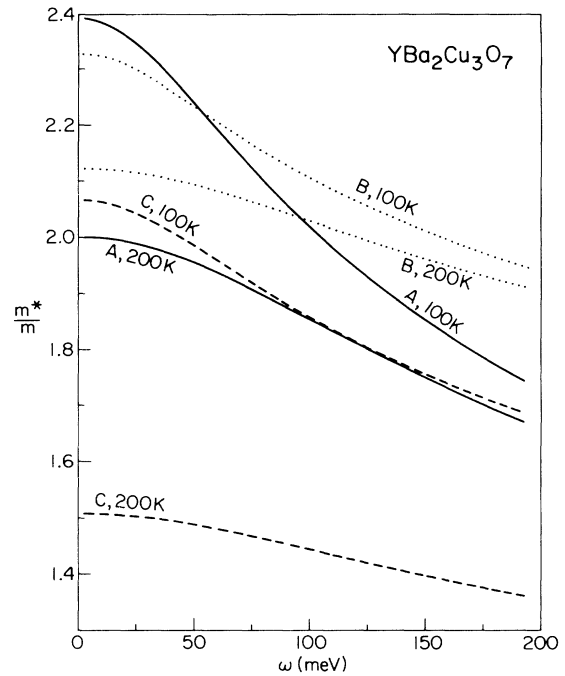


FIG. 5. Same as Fig. 3 but using  $g_0$  instead of  $g_s$ .

ment they obtain seems to be a little bigger than what the experiment suggests.

**B.  $\text{YBa}_2\text{Cu}_3\text{O}_{6.63}$**

In the case of  $\text{YBa}_2\text{Cu}_3\text{O}_{6.63}$  material with  $T_c = 60$  K, we are not aware of any experimental data on its optical

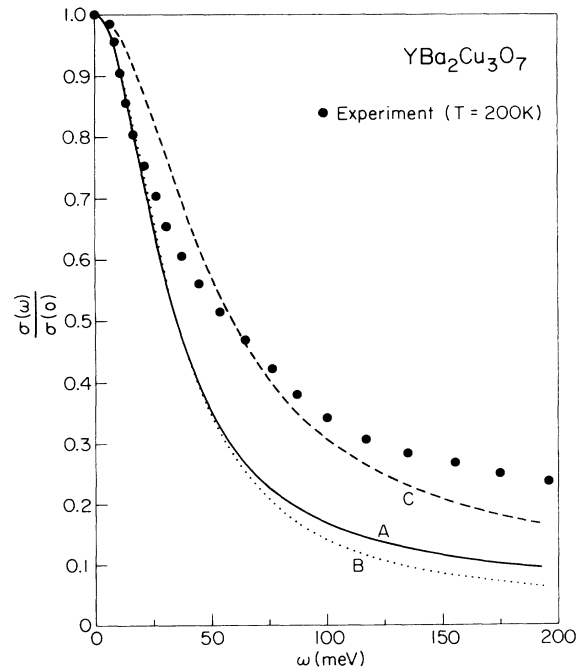


FIG. 6. Optical conductivity divided by its zero-frequency value,  $T = 200$  K for the three models compared to the experimental result of Ref. 7 for  $\text{YBa}_2\text{Cu}_3\text{O}_7$ .

properties. Orenstein *et al.* published data on  $T_c = 50$  K material. To evaluate the quantity  $g$ , in this case, we therefore use the value of  $\rho(T_c = 60 \text{ K}) = 240 \mu\Omega \text{ cm}$  given in Ref. 7, and we estimate  $\rho_{\text{SF}}(T_c) = 20 \mu\Omega \text{ cm}$ . Using the same reference we approximate  $\omega_p^* = 1.12 \text{ eV}$ . One of the striking properties of  $\text{YBa}_2\text{Cu}_3\text{O}_{6+x}$  materials is that as soon as one moves away from  $x = 1$  to smaller values,  $\chi_0$  becomes temperature dependent. Using  $\omega_p^* = 1.12 \text{ eV}$  and  $\rho_{\text{SF}}(T_c) = 20 \mu\Omega \text{ cm}$ , we obtain  $\alpha_0 \approx 0.22$  and

$$\begin{aligned} g &= 0.66, \text{ paramagnon,} \\ g &= 0.42, \text{ model B,} \\ g &= 0.32, \text{ model C.} \end{aligned} \quad (53)$$

In Figs. (7–10) we display our results for the  $T_c = 60$  K material. Most of the features described in the case of the  $T_c = 90$  K material remain valid, i.e., the linearity of the effective relaxation rate as a function of frequency, the weak frequency dependence of the mass enhancement, and the decreasing of  $\sigma(0)$  with increasing temperature. Still, there are some additional features. Two important differences are readily noticeable. Firstly, the magnitude of the mass enhancement at low frequencies for the  $T_c = 90$  K material is nearly twice that of the  $T_c = 60$  K material. Secondly, the variation with temperature is just the opposite in the two cases. For the  $T_c = 90$  K material,  $m^*/m$  decreases with temperature, while for  $T_c = 60$  K it increases except in the model C case, where we still have the same behavior. In our calculation, the main qualitative difference between the two models resides in the temperature dependences of  $\omega_{\text{SF}}$  and  $\chi_0(T)$ . Most probably, the difference between  $\omega_{\text{SF}}$  for the two cases has a minor impact on the mass enhancement as opposed to  $\chi_0(T)$ , since the mass enhancement is

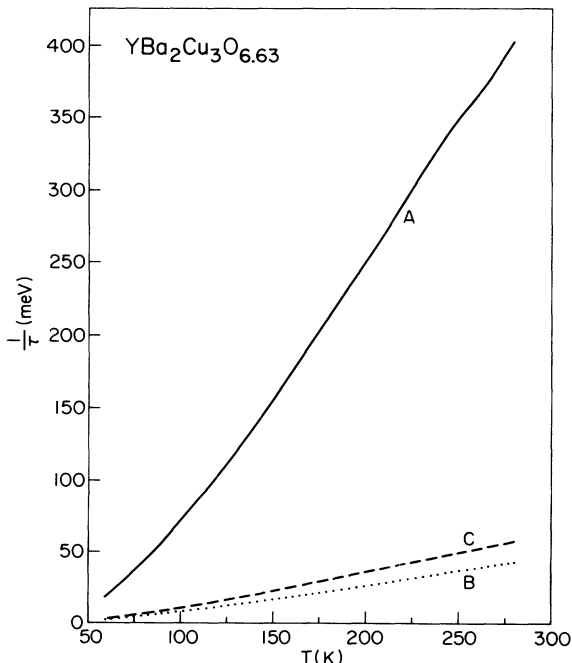


FIG. 7. Same as Fig. 1 but for  $\text{YBa}_2\text{Cu}_3\text{O}_{6.63}$  using  $g_0$ 's.

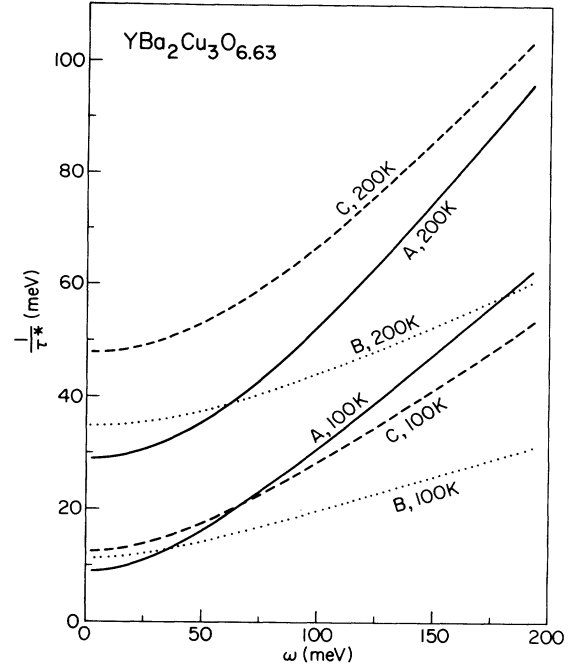


FIG. 8. Same as Fig. 2 but for  $\text{YBa}_2\text{Cu}_3\text{O}_{6.63}$  using  $g_0$ 's.

directly proportional to  $\chi_0(T)$ . It would be very helpful to verify this prediction experimentally for  $\text{YBa}_2\text{Cu}_3\text{O}_{6.63}$  by measuring on the same sample both the optical conductivity (from which  $m^*/m$  could be deduced as is done in Ref. 6) and  $\chi_0(T)$  and check whether there is any scaling between the two quantities at a fixed frequency.

## V. CONCLUSION

In this paper we have calculated the optical conductivity in the normal state of the cuprate superconductor

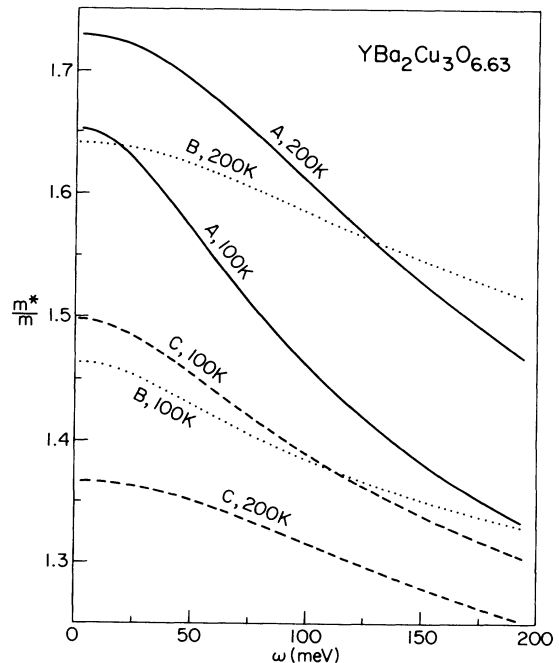


FIG. 9. Same as Fig. 3 but for  $\text{YBa}_2\text{Cu}_3\text{O}_{6.63}$  using  $g_0$ 's.

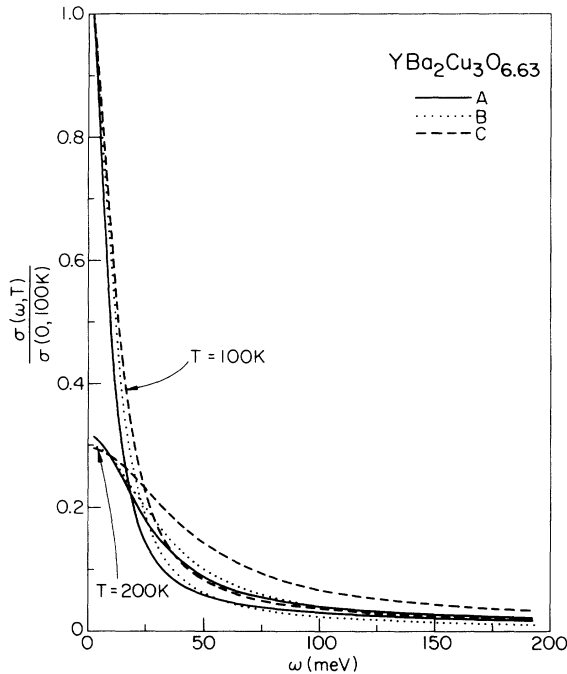


FIG. 10. Frequency dependence of the optical conductivity at  $T = 100$  and  $200$  K divided by its value at zero frequency and  $T = 100$  K, for the three models for  $\text{YBa}_2\text{Cu}_3\text{O}_{6.63}$  using respective  $g_0$ 's.

$\text{YBa}_2\text{Cu}_3\text{O}_{6+x}$  ( $x = 1, 0.63$ ). We also calculated the frequency dependence of the effective relaxation rate of the carriers as well as the mass enhancement. Our calculation is based on a phenomenological form for the spin susceptibility  $\chi$ . We propose three different forms of  $\chi$ . It turns out that each form produces the right behavior

of  $\sigma(\omega)$  in a certain range of frequency. Hence, one would like to compile a single form that interpolates between the frequency regions.

The results we obtain for  $\text{YBa}_2\text{Cu}_3\text{O}_7$  reproduce fairly well the linear behavior of the relaxation rate experimentally seen as a function of frequency, as well as the linear behavior of the dc relaxation rate as a function of temperature. We also find quite good agreement with the experimentally obtained mass-enhancement of the free carriers. The experimental data on the frequency dependence of the optical conductivity is roughly fitted by our calculation if we use model A or model B at small frequencies ( $\omega \leq 30$  meV), and model C for frequencies  $\omega \geq 50$  meV. In the case of  $\text{YBa}_2\text{Cu}_3\text{O}_{6.63}$ , we predict that the mass enhancement at a fixed frequency, but as a function of temperature, scales with the uniform static susceptibility. We also predict that the linearity of the effective relaxation rate as a function of frequency observed for  $\text{YBa}_2\text{Cu}_3\text{O}_7$  should persist for  $\text{YBa}_2\text{Cu}_3\text{O}_{6.63}$ .

This calculation can be improved in many ways. Instead of using a two-dimensional system one can include some hopping effects in the third dimension to simulate the real three-dimensional character of  $\text{YBa}_2\text{Cu}_3\text{O}_{6+x}$ . We have used a cylindrical Fermi surface; one could instead use a more realistic one. The other direction of improvement might be the inclusion of phonons in the picture by allowing the free carriers to interact with them.

#### ACKNOWLEDGMENTS

The author is thankful to Professor D. Pines for suggesting this problem to him and for many interesting discussions. He is also thankful to Dr. J. P. Lu, Dr. A. J. Millis, Dr. H. Monien, and P. Monthoux for so many interesting discussions. This work was supported by NSF Grant No. DMR89-20538.

<sup>1</sup>For a review see *The Los Alamos Symposium-1989: High Temperature Superconductivity Proceedings*, edited by K. S. Bedell, D. Coffey, D. E. Meltzer, D. Pines, and J. R. Schrieffer (Addison-Wesley, Reading, MA, 1990).  
<sup>2</sup>A. J. Millis, H. Monien, and D. Pines, *Phys. Rev. B* **42**, 167 (1990).  
<sup>3</sup>H. Monien, D. Pines, and M. Takigawa, *Phys. Rev. B* **43**, 258 (1991); H. Monien, P. Monthoux, and D. Pines, *ibid.* **43**, 275 (1991).  
<sup>4</sup>T. Moriya, and Y. Takahashi (unpublished).  
<sup>5</sup>F. Slakey, M. V. Klein, J. P. Rice, and D. M. Ginsberg, *Phys. Rev. B* **43**, 3764 (1991).  
<sup>6</sup>Z. Schlesinger, R. T. Collins, F. Holtzberg, C. Field, and S. H.

Blanton, *Phys. Rev. Lett.* **65**, 801 (1990).

<sup>7</sup>J. Orenstein, G. A. Thomas, A. J. Millis, S. L. Cooper, D. H. Raphine, T. Tikmusk, L. F. Schneemeyer, and J. V. Waszczak, *Phys. Rev. B* **42**, 6352 (1990).

<sup>8</sup>F. Gao, G. L. Carr, C. D. Porter, D. B. Tanner, S. Etemad, T. Venkatesan, A. Inam, B. Dutta, X. D. Wu, G. P. Williams, and C. J. Hirschmugl *Phys. Rev. B* **43**, 10383 (1991).

<sup>9</sup>W. Götze and P. Wölfle, *Phys. Rev. B* **6**, 1226 (1972).

<sup>10</sup>M. Takigawa, A. P. Reyes, P. C. Hammel, J. D. Thompson, R. H. Heffner, Z. Fisk, and C. Ott, *Phys. Rev. B* **43**, 247 (1991).

<sup>11</sup>J. Ruvalds and A. Virosztek, *Phys. Rev. B* **43**, 5498.